Hierarchical hollow nanoprisms based on ultrathin Ni-Fe layered double hydroxide nanosheets with enhanced electrocatalytic activity towards oxygen evolution

Yu, Le; Yang, Jing Fan; Guan, Bu Yuan; Lu, Yan; Lou, David Xiong Wen

2017

Yu, L., Yang, J. F., Guan, B. Y., Lu, Y., & Lou, D. X. W. (2018). Hierarchical hollow nanoprisms based on ultrathin Ni-Fe layered double hydroxide nanosheets with enhanced electrocatalytic activity towards oxygen evolution. Angewandte Chemie International Edition, 57(1), 172-176. doi:10.1002/anie.201710877

https://hdl.handle.net/10356/137733

https://doi.org/10.1002/anie.201710877

Hierarchical Hollow Nanoprisms Organized by Ultrathin Ni-Fe Layered Double Hydroxide Nanosheets with Enhanced Electrocatalytic Activity Toward Oxygen Evolution

Le Yu, Jing Fan Yang, Bu Yuan Guan, Yan Lu and Xiong Wen (David) Lou[*]

[*] Dr. L. Yu, J. F. Yang, Dr. B. Y. Guan, Dr. Y. Lu, Prof. X. W. Lou

School of Chemical and Biomedical Engineering, Nanyang Technological University, 62 Nanyang Drive, Singapore 637459, Singapore

Email: xwlou@ntu.edu.sg; davidlou88@gmail.com

Webpage: http://www.ntu.edu.sg/home/xwlou/

Abstract

Oxygen evolution reaction (OER) is involved in various renewable energy systems such as water splitting cells and metal-air batteries. Ni-Fe layered double hydroxides (LDHs) have been reported as promising OER electrocatalysts in alkaline electrolytes. The rational design of advanced nanostructures for Ni-Fe LDHs is highly desirable to optimize their electrocatalytic performance. Herein we report a facile self-templated strategy to synthesize novel hierarchical hollow nanoprisms composed of ultrathin Ni-Fe LDH nanosheets. Tetragonal nanoprisms of nickel precursors are first synthesized as the self-sacrificing template. Afterwards, these Ni precursors are consumed during the hydrolysis of iron(II) sulfate to simultaneously grow a layer of Ni-Fe LDH nanosheets around the surface. The resultant Ni-Fe LDH hollow prisms with large surface area manifest high electrocatalytic activity toward OER with low overpotential, small Tafel slope and remarkable stability.

Key words: Ni-Fe, layered double hydroxide, hollow, nanosheets, oxygen evolution reaction.

The fast depletion of fossil fuels and consequent cause of environmental problems have stimulated the research and development of renewable energy systems.[1-3] Specially, electrochemical water splitting is considered as a promising approach to obtain clean fuels from renewable but intermittent energy sources.[4,5] However, the realization of a fully integrated water-splitting system is largely hindered by the sluggish anodic oxygen evolution reaction (OER).[6] In this regard, an appropriate catalyst is necessary to accelerate the OER under low overpotentials (η) for enhanced energy conversion efficiency.[7,8] Many research efforts have been made to develop cost-effective electrocatalysts to replace the state-of-the-art precious metal based catalysts.[9-19]

Among various promising alternatives, oxides/hydroxides containing first row transition metals (Mn, Fe, Co and Ni etc.) have attracted tremendous interest owing to their earth-abundant nature and remarkable OER performance.[12-19] In particular, Ni-Fe layered double hydroxides (LDHs) have been reported as a promising class of the most effective OER catalysts under alkaline environment (pH = 13~14).[20-27] Although deep investigations for the identification of active sites are still needed, the synergistic interactions between Ni and Fe can indeed bring dramatic enhancement of catalytic activity compared with single Ni or Fe component.[28-33] As the OER process commonly takes place on the surface of a catalyst, the geometric structure of the electrocatalysts can strongly influence their activities.[12,34,35] Therefore, engineering nanostructures of Ni-Fe LDH based catalysts with targeted functionalities is highly desirable to further boost their OER activity by achieving high participation of electroactive species and facile transport of mass/electron in the catalytic process.

Hollow nanostructures have been widely designed as a unique type of advanced architectures in OER application due to their unique structural features.[34,36-39] Compared with bulk solid counterparts, hollow configurations with higher surface area usually endow catalysts with a higher density of surface exposed active sites. Moreover, their large void space could effectively reduce ionic transport resistance and ion diffusion length for the surface reactions.[34] Very recently, a few of pioneering works have demonstrated the successful generations of hollow nanostructured (oxy)hydroxides

toward water oxidation reaction with encouraging results.[37,38,40-46] For example, Yan and co-workers have reported the synthesis of α-$Ni(OH)_2$ hollow nanospheres through a template-free method.[40] The as-obtained hierarchical hollow nanospheres display enhanced OER activities compared with β-$Ni(OH)_2$ nanoplates/nanoparticles. In another case, Shi et al. have reported the preparation of VOOH hollow nanospheres through a similar hydrothermal strategy.[41] As an OER catalyst, the hollow structured VOOH exhibits smaller η compared with the solid control sample. Despite these advances, hard templates (e.g., SiO_2, Cu_2O) are usually involved to obtain hollow nanostructured catalysts with a uniform size distribution.[38,42] Facile self-engaged strategies without additional removal of inactive inner cores have become more and more attractive for preparing hollow electrocatalysts.[47,48]

Encouraged by these findings, we herein develop a self-templated strategy to fabricate hierarchical Ni-Fe LDH hollow nanoprisms assembled by ultrathin nanosheets. Solid prisms of nickel precursors are selected as the starting materials to provide the Ni source. After a fast and well-controlled hydrolysis of iron(II) sulfate, the coprecipitation process will generate an ultrathin Ni-Fe LDH shell around the prism-like core. Of note, the inner template can be simultaneously dissolved and transformed into active component without the removal step. Benefitting from the desirable compositions and prominent structural advantages, the as-obtained Ni-Fe LDH hollow nanostructures manifest enhanced electrocatalytic activity toward water oxidation reaction.

The straightforward synthesis of the novel Ni-Fe LDH hollow nanostructure is schematically depicted in **Figure 1**. We first fabricate prism-like Ni precursors as templates through a modified precipitation method. During the chemical transformation, the existence of water in the mixed solvent and protons generated from the hydrolysis of Fe^{2+} could gradually consume the templates to release the Ni^{2+} ions into the solution. At the same time, these released ions can participate in the precipitation of Fe^{2+} ions to form a hierarchical shell constructed from Ni-Fe LDH nanosheets at the surface of the Ni precursors. Then, the nanosheets continue to grow with the dissolution of inner core. Under a steady control of the solvent composition and Fe^{2+} ion concentration, a well-defined hierarchical Ni-

Fe LDH hollow nanoprisms can finally be obtained.

The panoramic field-emission scanning electron microscopy (FESEM) image indicates the template particles have a narrow size distribution with a prism-like configuration (**Figure 2**a). A closer FESEM observation further reveals a smooth surface over these whole prisms (Figure 2b). Besides, a uniform-contrast transmission electron microscopy (TEM) image of the Ni precursors demonstrates their solid and dense nature (Figure 2c). As illustrated by X-ray diffraction (XRD), the crystallographic structure of the Ni precursors is similar with the tetragonal cobalt acetate hydroxide (JCPDS card No. 22-0582) (Figure 2d).

After the hydrolysis reaction of iron(II) sulfate, the as-obtained discrete sample still preserves the prism-like morphology (**Figure 3**a). A magnified FESEM image clearly shows that the smooth surface of the prism-like precursor finally turns into a hierarchical shell constructed by randomly oriented nanosheets (Figure 3b). XRD pattern of the resultant hierarchical prisms can be assigned to a pure LDH phase, indicating the complete consumption of the Ni precursor template during the reaction (Figure S1, see Supporting Information). In addition, all the diffraction peaks are significantly broadened, which might be due to small crystallite size and stacking faults. Energy-dispersive spectroscopy (EDX) analysis validates the existence of Ni, Fe, C and S elements in these LDH prisms (Figure S2, see Supporting Information). Meanwhile, Fourier transform infrared (FTIR) spectrum indicates the co-existence of sulfate and acetate anions as the intercalating anions (Figure S3, see Supporting Information). As shown in Figure 3c, the interior cavity of these LDH prisms is clearly displayed by the sharp contrast between the hierarchical shell and the well-defined central void space. An enlarged TEM image verifies that the interconnected LDH nanosheets are loosely packed to form a highly porous texture (Figure 3d). Moreover, the visible dark strips are the folded edges or wrinkles of the nanosheets, indicating their ultrathin nature. Owing to these unique structural features, the Ni-Fe LDH hollow nanoprims exhibit a high Brunauer-Emmett-Teller (BET) specific surface area of 245.3 $m^2 g^{-1}$ (Figure S4, see Supporting Information). Besides, a set of distinct lattice

fringes with a spacing of 0.26 nm can be recognized in the shell, which is consistent with the (012) plane of LDH structure (Figure 3e). To investigate the spatial distribution of Ni and Fe elements, element mapping analysis under scanning transmission electron microscope (STEM) mode is carried out on an individual Ni-Fe LDH hollow particle. High-angle annular dark-field (HAADF)-STEM image and EDX mapping results confirm the uniform distribution of Ni and Fe elements throughout the hollow nanoframe (Figure 3f-i).

It is noteworthy that the solvent composition plays an imperative role in controlling the growth of the Ni-Fe LDH and the removal of the internal template during the hydrolysis reactions. More ethanol in the mixed solvent can slow down the transformation process. As a result, the Ni precursors are not dissolved completely and the released Ni^{2+} ions are not sufficient to support the growth of the newly formed Ni-Fe LDH nanosheets around the template surface (Figure S5a, see Supporting Information). Whereas, the reaction rate is accelerated with the increase of water content to form Fe-rich Ni-Fe LDH nanoclusters without prism-like appearance (Figure S5b and Figure S6, see Supporting Information). Besides, the morphology of the as-obtained sample could also be affected by the amount of Fe source. Specifically, a thin Ni-Fe LDH layer produced by insufficient Fe salt is not strong enough to withstand the outward mass transport during the dissolution of the inner template, leading to the collapse of the prism (Figure S7a, see Supporting Information). While, an excessive Fe dosage will generate some cluster-like by-products around the Ni-Fe LDH prisms (Figure S7b, see Supporting Information). When the usage of iron(II) sulfate is controlled in an appropriate range, the converted nanostructures exhibit similar hierarchical configurations composed by nanosheet subunits. Compared with the Ni-Fe LDH hollow prisms, the Ni-Fe LDH-10 (amount of iron(II) sulfate: 10 mg) sample shows lower Fe content and the other Ni-Fe LDH-50 (amount of iron(II) sulfate: 50 mg) sample has higher Fe/Ni atomic ratio (Figure S8, see Supporting Information).

Next, the water oxidation activities of the hierarchical Ni-Fe LDH hollow nanoprism electrocatalyst are investigated. **Figure 4**a presents the *iR*-compensated polarization curve.

Apparently, a redox peak around 1.4 V relative to the reversible hydrogen electrode (RHE) is observed, which is assigned to the oxidation process of Ni^{2+} to Ni^{3+}.[23,49] For OER performance evaluation, the operating potentials required at a current density (j) of 10 mA cm^{-2} are usually compared. In the present case, the anodic electrode based on the hierarchical hollow nanoprisms requires a small potential of 1.51 V (*vs.* RHE) to obtain the j of 10 mA cm^{-2}, corresponding to a low η of 280 mV. For comparison, the polarization curves of the control samples with *iR* correction are also investigated (Figure S9, see Supporting Information). As shown, the hierarchical Ni-Fe LDH hollow nanoprisms display apparent structural and compositional superiority with much higher catalytic activity over the Fe-rich Ni-Fe LDH nanoclusters, Ni-Fe LDH-10 and Ni-Fe LDH-50. Some previous studies have demonstrated that Ni and Fe elements have played vital roles in the control of active catalytic sites for Ni-Fe LDH, although further comprehensive study is still needed for the specific mechanism.[24,28,29] As indicated in Figure 4b, the linear portion of the Tafel plot is fitted into the Tafel equation ($\eta = b \log j + a$, where η is the overpotential, j is the current density, and b is the Tafel slope), yielding a small Tafel slope of 49.4 mV dec^{-1} for the hierarchical Ni-Fe LDH hollow nanoprisms.[20] Such high electrocatalytic activities of the Ni-Fe LDH hollow nanoprism product compare favorably to those of many high-performance Ni-Fe LDH based electrocatalysts (Table S1, see Supporting Information).[20,21,23,25,27,49,50] The enhanced performance might be ascribed to their unique hollow features and optimized chemical composition. Specifically, besides the synergistic effect between Ni and Fe elements, the hierarchical hollow nanoprisms with large surface area could provide sufficient electroactive sites for electrocatalytic reactions. As indicated by the cyclic voltammograms (CVs) in a proper potential range without redox processes and the corresponding capacitive current plots against the scan rate, the Ni-Fe LDH hollow nanoprism sample has much larger double-layer capacitance (C_{dl}) compared with the Ni-Fe LDH nanocluster catalyst, demonstrating the higher electrochemically active surface area (ECSA) of the hollow structure for the enhanced OER performance (Figure S10, see Supporting Information).

To avoid the potential physical loss of active materials on glassy carbon (GC) during high-speed rotating, these hollow structures are transferred onto Ni foam for the stability test. The contribution from the conductive substrate toward OER can be ignored due to its rather inferior activity (Figure S11, see Supporting Information). The long-term durability of these prism-like hollow nanostructures is tested by a chronopotentiometry (CP) measurement on Ni foam under the η of 295 mV. The obtained result demonstrates the j generally remains stable over 6 h with small degradation, corroborating the good stability in basic condition (Figure 4c). To further assess the stability of the Ni-Fe LDH hollow nanoprisms, consecutive CV scans are carried out. As seen from Figure 4d, CV curves show a small shift of about 10 mV at the j of 10 mA cm^{-2} after 1000 repeated cycles. Although the cycling causes considerable damage to the nanosheets, the overall structure of prisms is generally retained after the long-term stability test (Figure S12, see Supporting Information). The above experimental results suggest good stability of the Ni-Fe LDH hollow nanoprisms toward OER.

In summary, we have reported a facile self-engaged strategy to prepare hollow nanoprisms constructed by interconnected ultrathin Ni-Fe layered double hydroxide (LDH) nanosheets. With the steady control of hydrolysis process of iron(II) sulfate, prism-like Ni precursors can be dissolved and simultaneously converted to the final Ni-Fe LDH shell with tailorable chemical composition. Owing to the open and porous structural features and synergistic effect between Ni and Fe elements, the as-prepared hierarchical Ni-Fe LDH hollow nanoprisms manifest enhanced electrochemical performance toward the oxygen evolution reaction. Specifically, the electrode based on these hollow nanoprisms could reach a current density of 10 mA cm^{-2} at a small overpotential of 280 mV with a small Tafel slope of 49.4 mV per decade and excellent stability in alkaline electrolyte.

Acknowledgements

X. W. L. acknowledges the funding support from the National Research Foundation (NRF) of Singapore via the NRF investigatorship (NRF-NRFI2016-04).

References

[1] J. H. Montoya, L. C. Seitz, P. Chakthranont, A. Vojvodic, T. F. Jaramillo, J. K. Norskov, *Nat. Mater.* **2017**, *16*, 70.

[2] H. B. Zhang, J. W. Nai, L. Yu, X. W. Lou, *Joule* **2017**, *1*, 77.

[3] F. Y. Cheng, J. Chen, *Chem. Soc. Rev.* **2012**, *41*, 2172.

[4] Z. W. Seh, J. Kibsgaard, C. F. Dickens, I. B. Chorkendorff, J. K. Norskov, T. F. Jaramillo, *Science* **2017**, *355*, eaad4998.

[5] S. L. Zhao, Y. Wang, J. C. Dong, C. T. He, H. J. Yin, P. F. An, K. Zhao, X. F. Zhang, C. Gao, L. J. Zhang, J. W. Lv, J. X. Wang, J. Q. Zhang, A. M. Khattak, N. A. Khan, Z. X. Wei, J. Zhang, S. Q. Liu, H. J. Zhao, Z. Y. Tang, *Nat. Energy* **2016**, *1*, 16184.

[6] C. C. L. McCrory, S. H. Jung, J. C. Peters, T. F. Jaramillo, *J. Am. Chem. Soc.* **2013**, *135*, 16977.

[7] Y. Jiao, Y. Zheng, M. T. Jaroniec, S. Z. Qiao, *Chem. Soc. Rev.* **2015**, *44*, 2060.

[8] B. Y. Xia, Y. Yan, N. Li, H. B. Wu, X. W. Lou, X. Wang, *Nat. Energy* **2016**, *1*, 15006.

[9] J. T. Zhang, Z. H. Zhao, Z. H. Xia, L. M. Dai, *Nat. Nanotechnol.* **2015**, *10*, 444.

[10] Y. P. Zhu, C. X. Guo, Y. Zheng, S. Z. Qiao, *Acc. Chem. Res.* **2017**, *50*, 915.

[11] X. Xu, F. Song, X. L. Hu, *Nat. Commun.* **2016**, *7*, 12324.

[12] L. Han, S. J. Dong, E. K. Wang, *Adv. Mater.* **2016**, *28*, 9266.

[13] O. Diaz-Morales, I. Ledezma-Yanez, M. T. M. Koper, F. Calle-Vallejo, *ACS Catal.* **2015**, *5*, 5380.

[14] Y. P. Zhu, T. Y. Ma, M. Jaroniec, S. Z. Qiao, *Angew. Chem., Int. Ed.* **2017**, *56*, 1324.

[15] M. S. Burke, L. J. Enman, A. S. Batchellor, S. H. Zou, S. W. Boettcher, *Chem. Mater.* **2015**, *27*, 7549.

[16] B. Y. Guan, X. Y. Yu, H. B. Wu, X. W. Lou, *Adv. Mater.* **2017**, DOI: 10.1002/adma.201703614.

[17] M. Gorlin, P. Chernev, J. F. de Araujo, T. Reier, S. Dresp, B. Paul, R. Krahnert, H. Dau, P. Strasser, *J. Am. Chem. Soc.* **2016**, *138*, 5603.

[18] Y. Q. Zhang, B. Ouyang, J. Xu, G. C. Jia, S. Chen, R. S. Rawat, H. J. Fan, *Angew. Chem., Int. Ed.* **2016**, *55*, 8670.

[19] L. Chen, X. L. Dong, Y. G. Wang, Y. Y. Xia, *Nat. Commun.* **2016**, *7*, 11741.

[20] M. Gong, Y. G. Li, H. L. Wang, Y. Y. Liang, J. Z. Wu, J. G. Zhou, J. Wang, T. Regier, F. Wei, H. J. Dai, *J. Am. Chem. Soc.* **2013**, *135*, 8452.

[21] F. Song, X. L. Hu, *Nat. Commun.* **2014**, *5*, 4477.

[22] F. Dionigi, P. Strasser, *Adv. Energy Mater.* **2016**, *6*, 1600621.

[23] X. Long, J. K. Li, S. Xiao, K. Y. Yan, Z. L. Wang, H. N. Chen, S. H. Yang, *Angew. Chem., Int. Ed.* **2014**, *53*, 7584.

[24] M. Gong, H. J. Dai, *Nano Res.* **2015**, *8*, 23.

[25] B. M. Hunter, J. D. Blakemore, M. Deimund, H. B. Gray, J. R. Winkler, A. M. Muller, *J. Am. Chem. Soc.* **2014**, *136*, 13118.

[26] C. Tang, H. S. Wang, H. F. Wang, Q. Zhang, G. L. Tian, J. Q. Nie, F. Wei, *Adv. Mater.* **2015**, *27*, 4516.

[27] W. Ma, R. Z. Ma, C. X. Wang, J. B. Liang, X. H. Liu, K. C. Zhou, T. Sasaki, *ACS Nano* **2015**, *9*, 1977.

[28] L. Trotochaud, S. L. Young, J. K. Ranney, S. W. Boettcher, *J. Am. Chem. Soc.* **2014**, *136*, 6744.

[29] D. Friebel, M. W. Louie, M. Bajdich, K. E. Sanwald, Y. Cai, A. M. Wise, M. J. Cheng, D. Sokaras, T. C. Weng, R. Alonso-Mori, R. C. Davis, J. R. Bargar, J. K. Norskov, A. Nilsson, A. T. Bell, *J. Am. Chem. Soc.* **2015**, *137*, 1305.

[30] B. M. Hunter, W. Hieringer, J. R. Winkler, H. B. Gray, A. M. Muller, *Energy Environ. Sci.* **2016**, *9*, 1734.

[31] M. Görlin, J. Ferreira de Araújo, H. Schmies, D. Bernsmeier, S. Dresp, M. Gliech, Z. Jusys, P. Chernev, R. Kraehnert, H. Dau, P. Strasser, *J. Am. Chem. Soc.* **2017**, *139*, 2070.

[32] Y. Dong, P. X. Zhang, Y. L. Kou, Z. Y. Yang, Y. P. Li, X. M. Sun, *Catal. Lett.* **2015**, *145*, 1541.

[33] C. G. Morales-Guio, L. Liardet, X. L. Hu, *J. Am. Chem. Soc.* **2016**, *138*, 8946.

[34] G. Prieto, H. Tüysüz, N. Duyckaerts, J. Knossalla, G.-H. Wang, F. Schüth, *Chem. Rev.* **2016**, *116*, 14056.

[35] K. D. Gilroy, A. Ruditskiy, H. C. Peng, D. Qin, Y. N. Xia, *Chem. Rev.* **2016**, *116*, 10414.

[36] L. Yu, H. Hu, H. B. Wu, X. W. Lou, *Adv. Mater.* **2017**, *29*, 1604563.

[37] T. Kwon, H. Hwang, Y. J. Sa, J. Park, H. Baik, S. H. Joo, K. Lee, *Adv. Funct. Mater.* **2017**, *27*, 1604688.

[38] J. W. Nai, H. J. Yin, T. T. You, L. R. Zheng, J. Zhang, P. X. Wang, Z. Jin, Y. Tian, J. Z. Liu, Z. Y. Tang, L. Guo, *Adv. Energy Mater.* **2015**, *5*, 1401880.

[39] J. W. Nai, B. Y. Guan, L. Yu, X. W. Lou, *Sci. Adv.* **2017**, *3*, e1700732.

[40] M. R. Gao, W. C. Sheng, Z. B. Zhuang, Q. R. Fang, S. Gu, J. Jiang, Y. S. Yan, *J. Am. Chem. Soc.* **2014**, *136*, 7077.

[41] H. H. Shi, H. F. Liang, F. W. Ming, Z. C. Wang, *Angew. Chem., Int. Ed.* **2017**, *56*, 573.

[42] C. Zhang, M. F. Shao, L. Zhou, Z. H. Li, K. M. Xiao, M. Wei, *ACS Appl. Mater. Interfaces* **2016**, *8*, 33697.

[43] P. L. He, X. Y. Yu, X. W. Lou, *Angew. Chem., Int. Ed.* **2017**, *56*, 3897.

[44] B. Y. Guan, L. Yu, X. W. Lou, *Angew. Chem., Int. Ed.* **2017**, *56*, 2386.

[45] J. W. Nai, Y. Lu, L. Yu, X. Wang, X. W. Lou, *Adv. Mater.* **2017**, *29*, 1703870.

[46] K. Fan, Y. F. Ji, H. Y. Zou, J. F. Zhang, B. C. Zhu, H. Chen, Q. Daniel, Y. Luo, J. G. Yu, L. C. Sun, *Angew. Chem., Int. Ed.* **2017**, *56*, 3289.

[47] L. Yu, H. B. Wu, X. W. Lou, *Acc. Chem. Res.* **2017**, *50*, 293.

[48] X. J. Wang, J. Feng, Y. C. Bai, Q. Zhang, Y. D. Yin, *Chem. Rev.* **2016**, *116*, 10983.

[49] Y. Jia, L. Z. Zhang, G. P. Gao, H. Chen, B. Wang, J. Z. Zhou, M. T. Soo, M. Hong, X. C. Yan, G. R. Qian, J. Zou, A. J. Du, X. D. Yao, *Adv. Mater.* **2017**, *29*, 1700017.

[50] W. Zhang, Y. Z. Wu, J. Qi, M. X. Chen, R. Cao, *Adv. Energy Mater.* **2017**, *7*, 1602547.

Figures and Captions

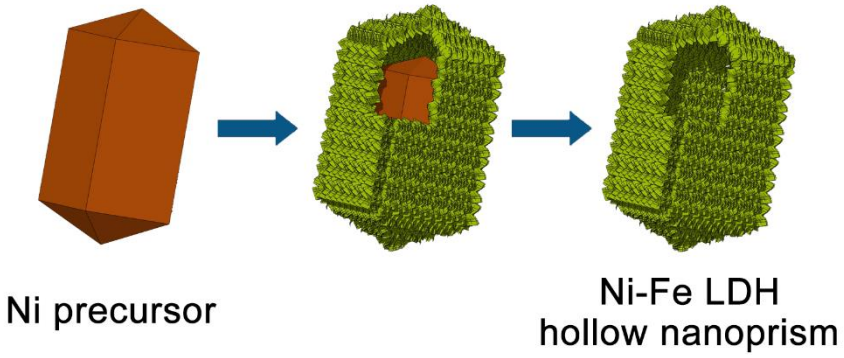

Figure 1. Schematic illustration on the formation of hierarchical Ni-Fe LDH hollow nanoprisms via a self-templated strategy.

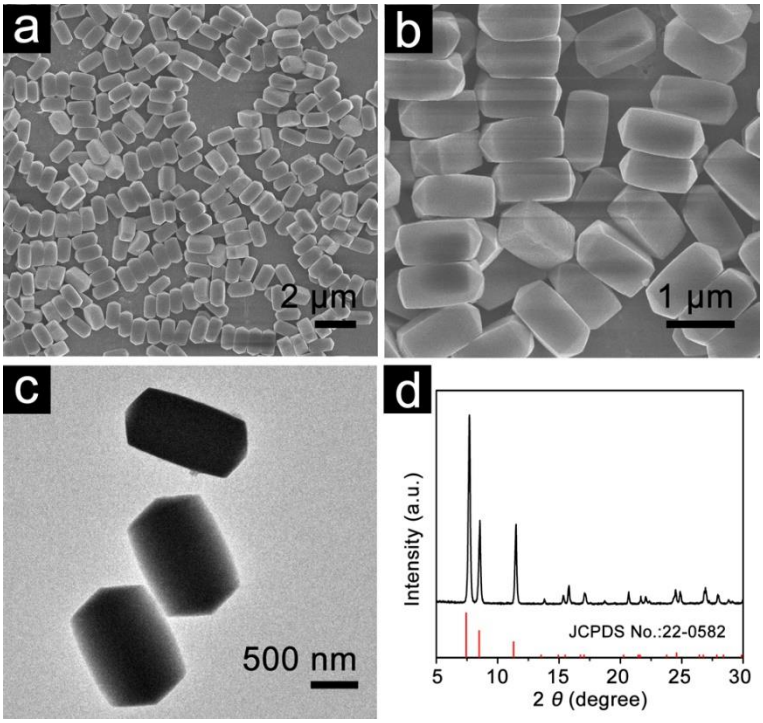

Figure 2. (a,b) FESEM images, (c) TEM image and (d) XRD pattern of prism-like Ni precursors.

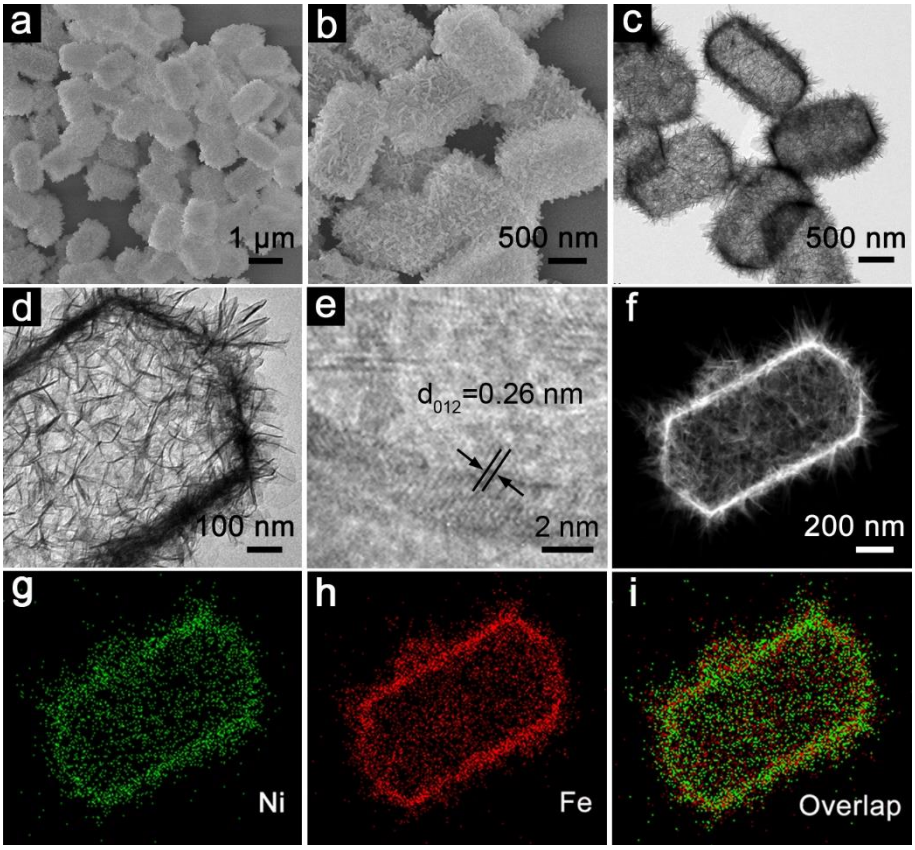

Figure 3. (a,b) FESEM and (c,d) TEM images of the hierarchical Ni-Fe LDH hollow prisms obtained after the hydrolysis reaction. (e) Lattice fringes from the Ni-Fe LDH shell. (f-i) HAADF-STEM image and elemental mapping images of an individual Ni-Fe LDH hollow prism.

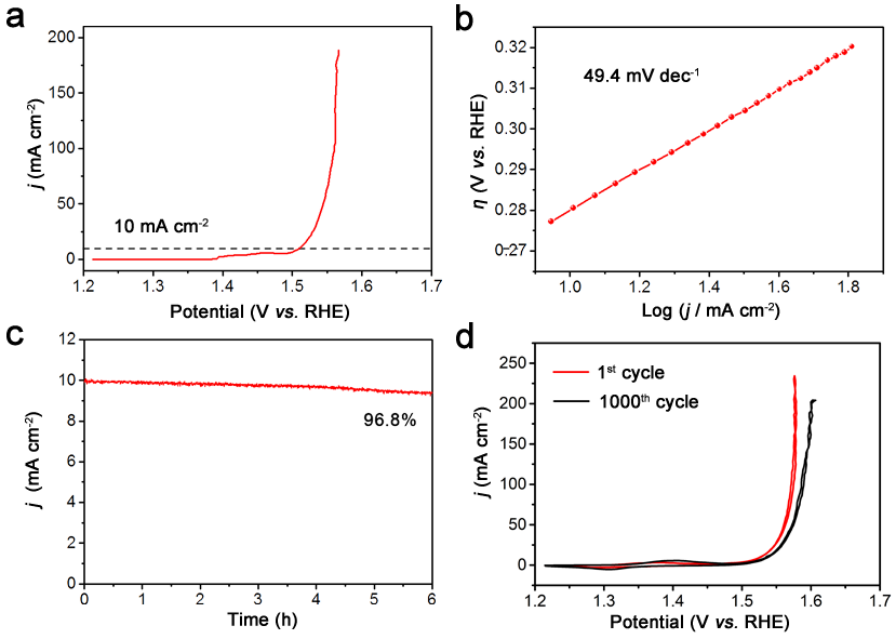

Figure 4. (a) Polarization curve and (b) Tafel plot of the Ni-Fe LDH hollow prisms on GC. (c) Time-dependent current density curve of the Ni-Fe LDH hollow prisms on Ni foam. (d) CV curves of the Ni-Fe LDH hollow prisms on Ni foam before and after 1000 repeated cycles.

for Table of Content Entry

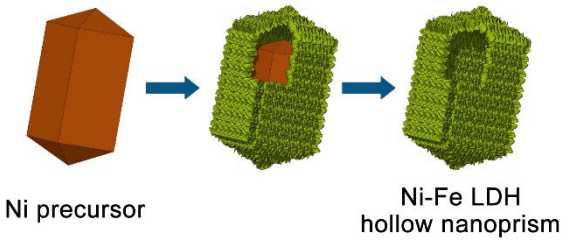

Hierarchical hollow nanoprisms composed of ultrathin Ni-Fe layered double hydroxide (LDH) nanosheets have been prepared via a facile self-templated strategy. During the hydrolysis process of iron(II) sulfate, prism-like Ni precursors can be dissolved and converted to a shell of Ni-Fe LDH around the surface. Due to the structural and compositional advantages, these well-defined hierarchical hollow nanoprisms manifest enhanced electrochemical activity as an electrocatalyst for oxygen evolution.